Taylor & Francis
Taylor & Francis Group

Journal of Asian Architecture and Building Engineering

ISSN: 1346-7581 (Print) 1347-2852 (Online) Journal homepage: https://www.tandfonline.com/loi/tabe20

Seismic Response of Base-isolated CRLSS Considering Nonlinear Elasticity of Concrete

Xuansheng Cheng, Liang Ma, Aijun Zhang & Bo Liu

To cite this article: Xuansheng Cheng, Liang Ma, Aijun Zhang & Bo Liu (2018) Seismic Response of Base-isolated CRLSS Considering Nonlinear Elasticity of Concrete, Journal of Asian Architecture and Building Engineering, 17:3, 533-540, DOI: 10.3130/jaabe.17.533

To link to this article: https://doi.org/10.3130/jaabe.17.533

Seismic Response of Base-isolated CRLSS Considering Nonlinear Elasticity of Concrete

Xuansheng Cheng*[1], Liang Ma[2], Aijun Zhang[3] and Bo Liu[4]

[1] Professor, School of Civil Engineering, Lanzhou University of Technology, China
[2] Research Associate, School of Civil Engineering, Lanzhou University of Technology, China
[3] Research Associate, School of Civil Engineering, Lanzhou University of Technology, China
[4] Research Associate, School of Civil Engineering, Lanzhou University of Technology, China

Abstract

The purpose of this paper is to study the seismic response of a base-isolated, concrete rectangular liquid-storage structure (CRLSS) under small-amplitude sloshing. In this study, the three-dimensional FEM of the base isolated CRLSS is established by using ADINA. The concrete material is assumed to be nonlinear and elastic, and the criterion for the small amplitude sloshing is defined to determine the seismic response of a base-isolated CRLSS under different conditions. The results show that when small-amplitude sloshing occurs and the nonlinear elasticity of the concrete material is considered, the displacement of wallboard, the height of liquid sloshing and the equivalent stress are increased with the increase in the earthquake intensity when comparing the same liquid height and different intensities of a bidirectional earthquake. The liquid height is found to affect the seismic response of the base-isolated CRLSS. The lower the liquid height is, the larger the equivalent stress is, and the greater the displacement of the wallboard and the amplitude of the liquid sloshing are.

Keywords: concrete; rectangular liquid-storage structure; nonlinear elasticity; liquid-solid interaction; seismic response

1. Introduction

Because liquid-storage structures are usually closely related to people's life and production, they are often placed in crowded urban areas. Because these structures are often located in populated areas, once this type of structure is damaged (due to, e.g., earthquake, terrorist attack, accidental impact), there may be high risks of potentially serious secondary disasters (e.g., fire, environment pollution, and explosions). Therefore, the research has been conducted on the seismic response of these liquid storage structures.

A new added mass approach was put forward by Balendra (1982), in which the internal liquid of the storage structure was represented by the added mass. Ju and Zeng (1983) studied this problem through the velocity potential function of fluid movement and obtained an analytical solution to the problem based on the assumption of a small-amplitude sloshing of the liquid. Andrianarison and Ohayon (2006) performed a theoretical study of the effect of gravity waves on a liquid storage structure. Li *et al.* (2002) analyzed the problem of the fluid-solid coupling dynamic response on a cylindrical liquid storage structure. Liu *et al.* (2005) analyzed the seismic response and seismic capacity of a rectangular liquid storage tank. Souli and Zolesio (2001) combined the least square method with a study on the sloshing effect of the internal liquid on a three-dimensional liquid storage structure subjected to external excitation. Yue *et al.* (2001) systematically studied the nonlinear characteristic of the liquid sloshing response of a liquid storage structure in a three-dimensional space by use of the Arbitrary Lagrangian Eulerian (ALE). Using the displacement potential flow equation of a finite element and considering the fluid-solid coupling effect, Zhang *et al.* (2011) studied the dynamic response of a liquid storage structure. Ayman A. Seleemah and Mohamed El-Sharkawy (2011) investigated the seismic response of elevated liquid storage tanks isolated by elastomeric or sliding bearings. Shi *et al.* (2012) studied the dynamic buckling performance of fluid-solid coupling about a large liquid-storage tank. Tao (2013) solved the unsteady fluid-structure interaction (FSI) problems with large structural displacement by partitioned solution approaches. Hashemi *et al.* (2013) put forward the analysis method of dynamic response of a three-dimensional rectangular liquid storage structure with elastic wallboard and studied the relationship between the structure parameters and the dynamic response. Yazici (2014) studied the effect of isolation parameters on the dynamic response of a liquid storage structure using the state-space method and concluded that

*Contact Author: Xuansheng Cheng, Professor,
School of Civil Engineering, Lanzhou University of Technology,
No. 287 Langongping Road, Lanzhou 730050, China
Tel: +86-931-2973784 Fax: +86-931-2976327
E-mail: chengxuansheng@gmail.com
(Received April 3, 2017 ; accepted July 23, 2018)
DOI http://doi.org/10.3130/jaabe.17.533

isolation measures can effectively reduce the shear of the foundation but that attention must be paid to the increase in the sloshing height caused by the isolation. Zhang *et al.* (2014) performed the shaking table experiment on a steel storage tank with multiple friction pendulum bearings. Moeindarbari *et al.* (2014) conducted the probabilistic analysis of a seismically isolated elevated liquid storage tank using multi-phase friction bearing. Malhotra *et al.* (2014) concluded that only 28% of the liquid movement would produce seismic force and that the remaining 72% of the liquid would slosh near the free surface and would not significantly influence the seismic force. Cheng *et al.* (2009; 2011; 2014; 2015) studied the liquid-solid coupling vibration characteristics of a rectangular liquid storage structure in theory.

In conclusion, although CRLSSs have been extensively studied in the existing literature, the nonlinear effect of concrete has not been considered. Therefore, in this paper, the nonlinear elastic property of concrete is considered. An integrated model of liquid-solid coupling dynamic analysis of CRLSS is established by studying the seismic effect on liquid sloshing height, wallboard displacement and equivalent stress of CRLSS. The variation laws of wave height, wallboard displacement and stress with different liquid levels are also analyzed.

2. Governing Equation

2.1 Boundary Condition of Free Liquid

Considering the small sloshing of a free surface, the boundary condition is

$$\frac{1}{g}\frac{\partial^2 p}{\partial t^2}+\frac{\partial p}{\partial z}=0 \tag{1}$$

where z is the vertical direction, g is the acceleration of gravity, t is time, and p is the liquid pressure.

2.2 Boundary Condition of Liquid–wallboard Interface

On the interface between the liquid and wallboard, there is no liquid flowing in the direction of the vertical wallboard, and the boundary condition is

$$\frac{\partial p}{\partial n}=-\rho a_n^s \tag{2}$$

where n is the normal direction of the wallboard and a_n^s is the acceleration acting on the liquid in the n direction.

2.3 Discrete Equation of Liquid Domain

Using the Galerkin method, the finite element discrete equation of fluid domain can be expressed as

$$\mathbf{G}\ddot{\mathbf{P}}+\mathbf{C}_f\dot{\mathbf{P}}+\mathbf{K}_f\mathbf{P}=\mathbf{F} \tag{3}$$

where

$$G_{ij}^e=\frac{1}{g}\int_{A_e}N_iN_j dA;$$

$$H_{ij}^e=\int_{V_e}\left(\frac{\partial N_i}{\partial x}\frac{\partial N_j}{\partial x}+\frac{\partial N_i}{\partial y}\frac{\partial N_j}{\partial y}+\frac{\partial N_i}{\partial z}\frac{\partial N_j}{\partial z}\right)dV;$$

$$\mathbf{F}=\mathbf{F}_i-\rho\mathbf{Q}^T\left(\ddot{\mathbf{U}}+\ddot{\mathbf{U}}_g\right);$$

$$F_i^e=\int_{A_e}N_i\frac{\partial p}{\partial n}dA\cdot$$

where N_i, $\ddot{U}$, $\ddot{U}_g$, Q and C_f are the shape function of node i of the liquid unit, the node acceleration of the structure, the ground acceleration, the interaction matrix and the damping matrix of the fluid domain, respectively.

2.4 Interaction Matrix

The interaction matrix Q can transfer the liquid pressure of the liquid-solid interaction interface to the wallboard in the form of a node force. The matrix can be obtained using the proportion agglomeration method. For an 8-node section element with translation freedom degree in the x, y and z directions and a 4-node section element of each node with pressure freedom degree, the interaction matrix can be expressed as (Mirzabozorg *et al.*, 2012)

$$\boldsymbol{Q}=\omega\int_{-1}^{1}\int_{-1}^{1}\begin{bmatrix}\alpha_1N_1^sN_1^f & & \alpha_1N_1^sN_4^f\\ \beta_1N_1^sN_1^f & & \beta_1N_1^sN_4^f\\ \gamma_1N_1^sN_1^f & & \gamma_1N_1^sN_4^f\\ & & \\ \alpha_8N_8^sN_8^sN_1^f & & \alpha_8N_8^sN_8^sN_4^f\\ \beta_8N_8^sN_8^sN_1^f & & \beta_8N_8^sN_8^sN_4^f\\ \gamma_8N_8^sN_8^sN_1^f & & \gamma_8N_8^sN_8^sN_4^f\end{bmatrix}_{24\times4}\left\|t_\xi\times t_\eta\right\|d\xi d\eta \tag{4}$$

where

$$t_\xi=\left\{\frac{\partial x}{\partial\xi},\frac{\partial y}{\partial\xi},\frac{\partial z}{\partial\xi}\right\}^T;\quad t_\eta=\left\{\frac{\partial x}{\partial\eta},\frac{\partial y}{\partial\eta},\frac{\partial z}{\partial\eta}\right\}^T;$$

$$\omega=\frac{A}{\sum_{i=1}^{8}\int_{A_e}N_i^sN_i^s\left|t_\xi\times t_\eta\right|d\xi d\eta};$$

$$A=\int_{A_e}\left\|t_\xi\times t_\eta\right\|d\xi d\eta\cdot$$

where N^f and N^s are the shape function of fluid domain and structure domain, respectively.

2.5 Damping Matrix of Fluid Domain

The damping matrix of the fluid domain is composed of a convection and a pulse (Mirzabozorg *et al.*, 2012) and can be expressed as

$$\boldsymbol{C}_f=a\boldsymbol{G}+b\boldsymbol{K}_f \tag{5}$$

where a and b can be calculated by the Rayliegh damping a can be obtained by the sloshing frequency of a free surface, and b can be obtained by the natural frequency of the structure wallboard.

3. Constitutive Relation of Concrete

In practical engineering, the growth rate of the concrete stress is significantly less than that of the strain in the load application process. Thus, in practical engineering, the nonlinear elastic modulus of concrete materials is usually used, and the relationship between the stress and strain can be expressed as

$$\sigma = E(\sigma)\varepsilon \tag{6}$$

where σ and ε are the stress and strain of the concrete, respectively, and E is the elastic modulus and is a function of stress, but is not a constant.

To obtain the solution conveniently, in this paper, the concrete constitutive model put forward by Sargin *et al.* is applied (Lv *et al.*, 1999):

$$\sigma = k_1 f_c \frac{F_1 \dfrac{\varepsilon}{\varepsilon_0} + (F_2 - 1)\left(\dfrac{\varepsilon}{\varepsilon_0}\right)^2}{1 + (F_2 - 1)\dfrac{\varepsilon}{\varepsilon_0} + F_2\left(\dfrac{\varepsilon}{\varepsilon_0}\right)^2} \tag{7}$$

where k_1 is the effect coefficient of lateral restraint on strength, f_c is the ultimate compressive strength of the prism, ε_0 is the strain corresponding to the ultimate compressive strength of the prism, and F_1 and F_2 are the strength parameters.

4. Determination of Small-amplitude Sloshing

In general, liquid sloshing is considered small-amplitude sloshing when the sloshing amplitude is no more than 1% of the liquid depth. Assuming that the sloshing of the liquid is linear under small-amplitude sloshing, basic theory can be used for the analysis. The liquid sloshing of CRLSS is a phenomenon that involves the mutual conversion between the liquid kinetic energy and the gravitational potential energy.

Considering the Bernoulli equation $p + \dfrac{\rho|U|^2}{2} + \rho g\eta = c$, the condition $|U|^2 \ll g\eta$ is satisfied. Namely, the liquid sloshing is linear, neglecting the nonlinear square term (Liu and Huang, 1993), the response frequency of liquid sloshing is ω_r, and the movement rate $|U|$ is approximately equal to $|\omega\eta|$ in magnitude; thus,

$$|\eta| \le \frac{2\varepsilon g}{\omega_r^2} \tag{8}$$

where $\dfrac{2\varepsilon g}{\omega_r^2}$ is defined as the critical amplitude η_0. If the sloshing amplitude is less than the critical amplitude, namely, $|\eta| < |\eta_0|$, the small-amplitude hypothesis can be used. However, if the sloshing amplitude exceeds the critical amplitude, namely, $|\eta| < |\eta_0|$, the nonlinear term $\dfrac{1}{2}|U|^2$ of the Bernoulli equation must be considered. For liquid, the critical amplitude is decided by the sloshing frequency, and the influence of the external excitation on the response frequency of the liquid storage is small when the sloshing is linear and the amplitude is small. Therefore, the response frequency can be replaced by the natural frequency of the corresponding modal, which is

$$\eta_0 = \frac{2\varepsilon g}{\omega_0^2} \tag{9}$$

Therefore, as long as the natural frequency of the liquid sloshing is calculated, the limit wave height under small amplitude sloshing and large-amplitude sloshing can be obtained. The natural frequency can be obtained directly by the dispersion equation of ideal potential fluid, which is

$$\omega_0^2 = \frac{n\pi g}{2b}\tanh\left(\frac{n\pi d}{2b}\right) \tag{10}$$

where n is the nth order modality, d is the liquid depth, and b is the wallboard width of the liquid storage structure.

5. Calculation Model and Calculation Parameter

5.1 Calculation Model

An isolated CRLSS that is positioned over land and does not have a top plate is the model selected for analysis in this paper. The length, width and height of the structure are all 6 m, the thicknesses of the wallboard and soleplate are both 0.3 m, the height of the liquid in the structure is 4 m, and the isolation layer thickness of the rubber pad is 0.2 m.

A 3D-solid unit is adopted as the structure unit, and the fluid is assumed to be the potential flow unit. Considering the effect of gravity waves, the fluid surface is defined as a free liquid surface. By dividing the structure, the fluid and the rubber isolation body into uniform grids, the grid density is set at 0.15 m, and the 8-node format is selected to divide the element.

Substituting the relevant data into Eq. (8), we can obtain $\tilde{\omega}_n^2$ =0.1998 rad/s. Substituting it into Eq. (9), we can obtain H=0.50 m. Therefore, in this study, the dynamic response of the CRLSS is considered when the wave height of the liquid sloshing is less than 0.50 m.

5.2 Calculation Parameter

(1) Rubber isolation cushion

To describe the hyper-elastic constitutive model of rubber, the strain energy density function obtained by Mooney-Rivlin (Zheng *et al.*, 2003; Huang *et al.*, 2008) is used. The strain energy density function W, as described by the invariant of deformation tensor, is

$$W = \sum_{i+j-1}^{n} C_{ij}(I_i - 3)^i (I_j - 3)^j \tag{11}$$

where, C_{ij} is the material constant, generally determined by experiments. I is the deformation tensor invariant.

All rubber supports are established through the 3D-Solid unit. According to the material constants reported in the literature (Liu *et al.*, 2011), the parameters of the Mooney-Rivlin rubber model are shown in Table 1.

Table 1. Parameters of Mooney-Rivlin Rubber Model

C1	C2	C3	C4	C5	C6
807300	168900	0	0	0	0

(2) Concrete

For concrete with a tensile strength of 30 MPa, f_c is 14.3 MPa, ε_0 is 0.002, k_1 is 1, F_1 is 1.7388, and F_2 is 0.5.

(3) Fluid

Because the object of the study is small-amplitude sloshing, the liquid is considered a potential fluid, and the bulk modulus of the liquid is 2.3×10^9 Pa. The density of the liquid is 1000 kg/m^3.

6. Dynamic Responses

The liquid storage structure is analyzed by using the El Centro seismic wave. The seismic wave record of 30 s is taken, and the bi-directional horizontal seismic wave is input in the x and y directions. The change in the liquid sloshing displacement, wallboard displacement, and structure stress of the CRLSS with seismic fortification intensities of 7, 8 and 9 are considered.

6.1 Seismic Response of Same Liquid Height

(1) Wallboard displacement

Under small-amplitude sloshing, when the numerical simulation is carried out on the isolated CRLSS, considering the nonlinear elasticity of concrete, and the waves of frequent seismic fortification intensities 7, 8 and 9 are input in the x direction and y directions, the wallboard displacement of the CRLSS is shown in Fig.1., and the peak displacement of the wallboard under the seismic effect is shown in Table 2.

From Fig.1., it can be clearly seen that when considering the nonlinear elastic characteristic of concrete, the peak displacement of the isolated CRLSS appears at the edge of the top of the wallboard when seismic fortification intensities are 7, 8 or 9. It can also be seen that the peak displacement of the wallboard is different when different seismic intensities are applied and that the peak displacement of the wallboard of the CRLSS increases continuously with the increase in seismic intensity.

(2) Liquid sloshing height

When the frequent seismic fortification intensities are 7, 8 or 9, the horizontal seismic wave is input in the x and y directions to the CRLSS. Considering the nonlinear elasticity of concrete, the change in liquid sloshing height of the isolated CRLSS is shown in Fig.2., and the peak height of the liquid sloshing wave is shown in Table 3.

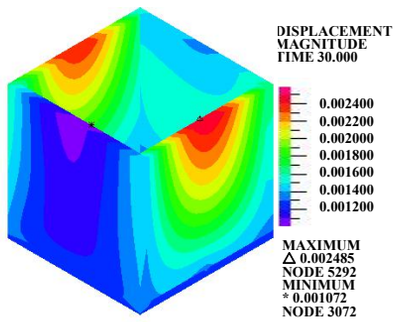

(a) Seismic fortification intensity 7

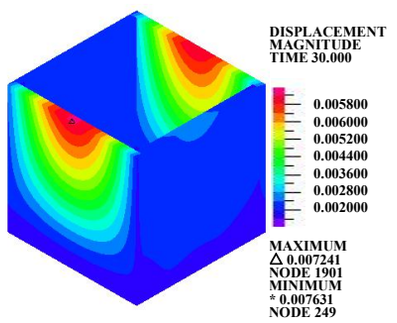

(b) Seismic fortification intensity 8

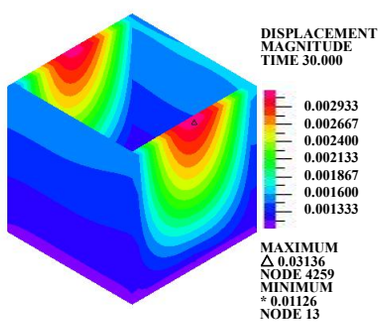

(c) Seismic fortification intensity 9

Fig.1. Wallboard Displacement

Table 2. Peak Displacement of Wallboard/m

Seismic fortification intensity	7	8	9
Peak displacement	0.002485	0.007241	0.03136

From Fig.2. and Table 3., when the nonlinear elasticity of concrete is considered in the effect of frequent bidirectional seismic waves, the peak liquid shaking height of the isolated CRLSS is different with different seismic intensities, and the liquid sloshing amplitude increases continuously with the increase of seismic intensity.

(3) Equivalent stress

When the frequent seismic fortification intensities are 7, 8 or 9, the bi-directional horizontal seismic wave is input to the CRLSS, considering the nonlinear elasticity of concrete; the change in the equivalent stress of the isolated CRLSS is shown in Fig.3. The equivalent stress peak of the CRLSS is shown in Table 4.

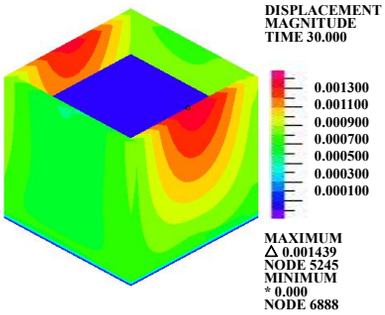

(*a*) Seismic fortification intensity 7

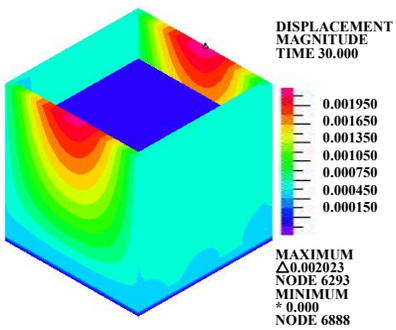

(b) Seismic fortification intensity 8

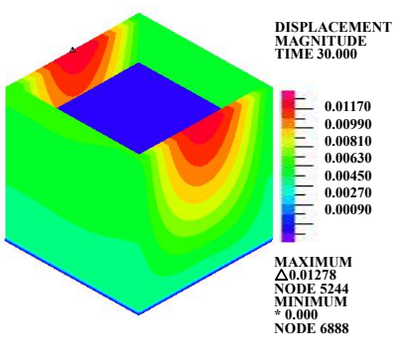

(c) Seismic fortification intensity 9

Fig.2. Liquid Sloshing Height

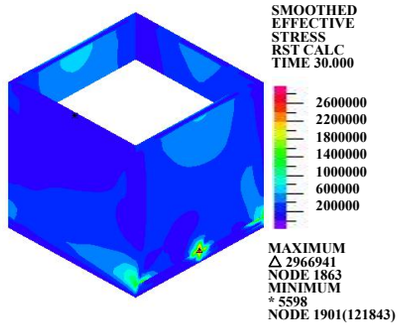

(*a*) Seismic fortification intensity 7

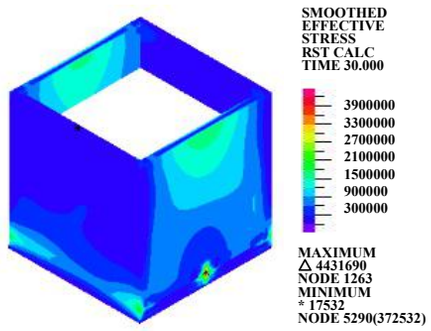

(b) Seismic fortification intensity 8

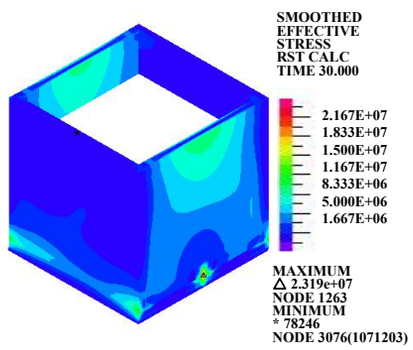

(c) Seismic fortification intensity 9

Fig.3. Equivalent Stress

Table 3. Peak Height of Liquid Shaking/m

Seismic fortification intensity	7	8	9
Peak shaking	0.001439	0.002023	0.01278

From Fig.3. and Table 4., the equivalent stress peak of frequent seismic fortification intensities for 7, 8 or 9 appear in the middle of the bottom of the wallboard, and the equivalent stress increases continuously with the increase in seismic intensity.

6.2 Seismic Response with Different Liquid Heights

To study the seismic response of the liquid-solid interaction of the nonlinear isolated CRLSS with different liquid heights, the liquid heights selected are 4 m, 3 m and 2 m, and a rare earthquake wave, the El-Centro wave, with a seismic fortification intensity of 7 in the *y*-direction is added.

Table 4. Peak Value of Equivalent Stress/Pa

Seismic fortification intensity	7	8	9
Peak equivalent stress	2966941	4431690	23190000

When the liquid appears to have small-amplitude sloshing, considering the nonlinear elasticity of concrete, under the unidirectional earthquake of a rare El-Centro wave of seismic fortification intensity of 7 and with different liquid levels, the wallboard displacement, liquid shaking and equivalent stress of the isolated CRLSS are obtained as shown in Figs.5., 6. and 7. Then, based on Figs.4., 5. and 6., the peak values of the seismic responses of the different liquid levels are shown in Table 5.

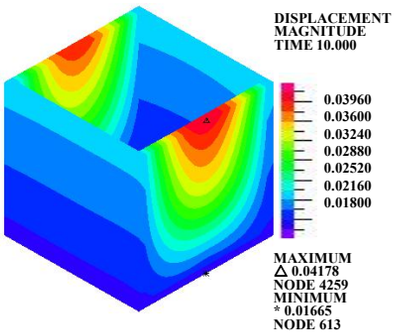

(a) 4 m

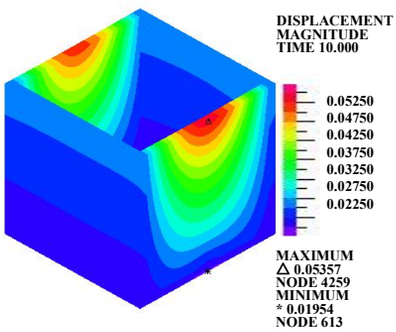

(b) 3 m

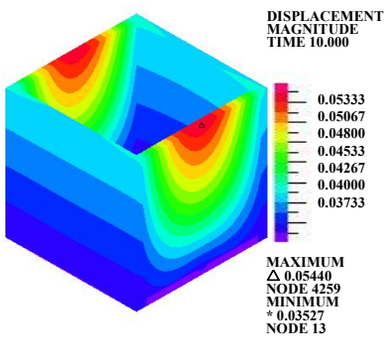

(c) 2 m

Fig.4. Wallboard Displacement

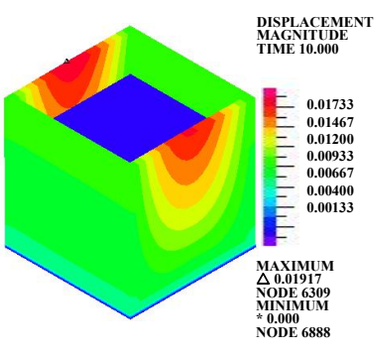

(a) 4 m

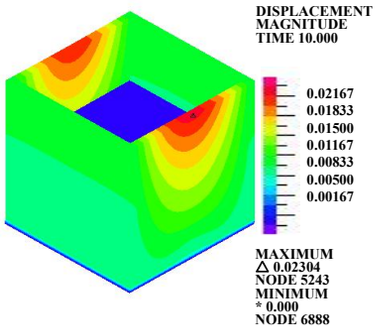

(b) 3 m

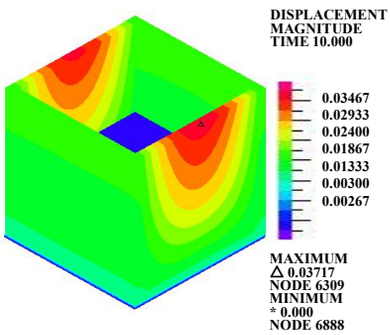

(c) 2 m

Fig.5. Liquid Shaking Height

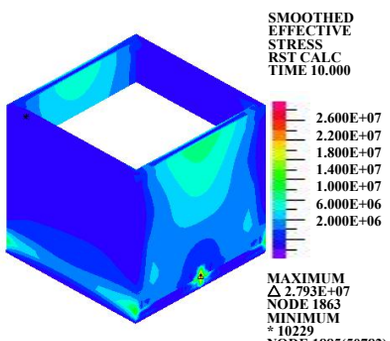

(a) 4 m

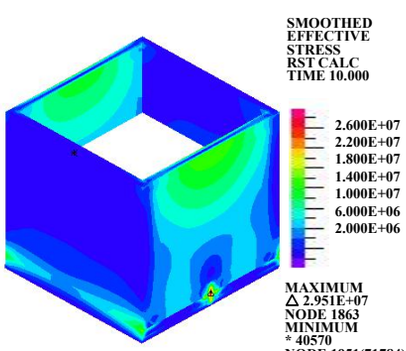

(b) 3 m

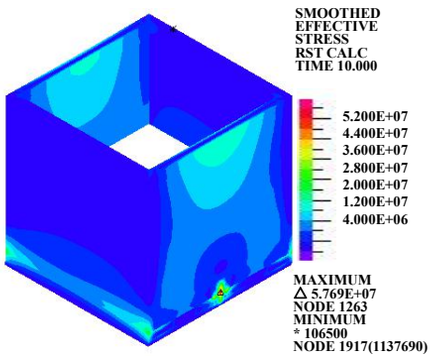

(c) 2 m

Fig.6. Equivalent Stress

Table 5. Peak Value of Seismic Response with Different Liquid Heights

Liquid height (m)	Wallboard displacement (m)	Liquid shaking height (m)	Equivalent stress (Pa)
4	0.04178	0.01917	2.793E+07
3	0.05357	0.02304	2.951E+07
2	0.05440	0.03717	5.769E+07

From Figs.5., 6., and 7. and Table 5., when the nonlinear elasticity of concrete is considered under small amplitude sloshing, the isolated CRLSS has different seismic responses under the same earthquake conditions and different liquid levels. The lower the liquid level is, the greater the change in stress, wallboard displacement and amplitude of liquid shaking are. In contrast, the higher the liquid level is and the greater the volume of liquid is, the smaller the liquid shaking amplitude, equivalent stress and wallboard displacement are for the isolated CRLSS.

7. Conclusions

(1) Due to the influence of frequency-domain and time-domain and the characteristics of the seismic waves under different earthquake intensities, the seismic response of the isolated CRLSS is different.

(2) When frequent bi-directional seismic action of different intensities are applied to the same liquid height, the wallboard displacement, the liquid shaking height and the equivalent stress of the isolated CRLSS increases continuously with the increase in seismic intensity.

(3) Different liquid levels influence the seismic response of the isolated CRLSS. The lower the liquid level is, the greater the change of equivalent stress, wallboard displacement and amplitude of liquid shaking. On the contrary, the higher the liquid level is and the greater the volume of liquid is, the smaller the liquid shaking amplitude, stress and wallboard displacement of the isolated CRLSS are.

Conflict of Interests

The authors declare that there is no conflict of interest regarding the publication of this paper.

Acknowledgments

This paper is a part of a part of the national natural science foundation of China (Grant number: 51368039), and a part of the plan project of science and technology in the Gansu province (Grant number: 144GKCA032).

References

1) Andrianarison, O., and Ohayon, R. (2006). Compressibility and gravity effects in internal fluid–structure vibrations: Basic equations and appropriate variational formulations. Computer Methods in Applied Mechanics Engineering, 195: 1958–1972, DOI: 10.1016/j.cma.2004.12.032.
2) Ayman A. Seleemah, and Mohamed El-Sharkawy (2011). Seismic analysis and modeling of isolated elevated liquid storage tanks. Earthquakes and Structures, An International Journal, 2(4): 397-412, DOI: 10.12989/eas.2011.2.4.397.
3) Balendra, T.A. (1982). Seismic design of flexible cylindrical liquid storage tanks. Earthquake Engineering and Structure Dynamics, 10(3): 477-496, DOI: 10.1002/eqe.4290100310.
4) Cheng, X.S., Cao, L.L., and Zhu, H.Y. (2015). Liquid-solid interaction seismic response of an isolated over ground rectangular reinforced-concrete liquid-storage structure. Journal of Asian Architecture and Building Engineering, 14(1): 175-180,DOI: http://doi.org/10.3130/jaabe.14.175.
5) Cheng, X.S. and Du, Y.F. (2009). The dynamic fluid pressure of reinforced concrete rectangular liquid-storage tanks with elastic walls. Engineering Mechanics, 26(6): 82-88, DOI: 1000-4750 (2009) 06-0082-07.
6) Cheng, X.S. and Du, Y.F. (2011). Vibration characteristic analysis of rectangular liquid-storage structures considering liquid-solid coupling on elastic foundation. Engineering Mechanics, 28(2): 186-192, DOI: 1000-4750 (2011) 02-0186-07.
7) Cheng, X.S., Li, P.J., Zhu, H.Y., Zhu, Q.K., Dang, Y., and Zhang, Q. (2014). The liquid–solid coupling seismic response of non-isolation overground rectangular reinforced concrete liquid-storage structures. China Civil Engineering Journal, 47(S): 42-47, DOI: 1000-131X (2014) S1- 0042-06.
8) Hashemi, S., Saadatpour, M.M., and Kianoush, M.R. (2013). Dynamic analysis of flexible rectangular fluid containers subjected to horizontal ground motion. Earthquake Engineering and Structural Dynamics, 42(11): 1637-1656, DOI: 10.1002/eqe.2291.
9) Huang, J.L., Xie, G.J., and Liu, Z.W. (2008). FEA of hyperelastic rubber material based on Mooney-Rivlin model and Yeoh model. China Rubber Industry, 8:467-472, DOI: 1000-890X (2008) 08-0467-05.
10) Ju, R.C., and Zeng, X.C. (1983). Coupling vibration theory of elastic structure and liquid. Seismological Press, Beijing.
11) Liu, Y.H., Wang, K.C., and Chen, H.Q. (2005). Seismic analysis of liquid storage container. Earthquake engineering and engineering vibration, 25(1): 149-154, DOI: 1000-1301 (2005) 01-0149-06.
12) Liu, M., Wang, Q.C., and Wang, G.Q. (2011). Determination of material constants of rubber Mooney-Rivlin model. China Rubber Industry, 58(4): 241-245, DOI: 1000-890 (2011) 04-0241-05.
13) Liu, Z.H. and Huang, Y.Y. (1993). An arbitrary lagrangian-eulerian boundary element method for large-amplitude sloshing problems. Journal of Vibration Engineering, 6(1): 10-18.
14) Li, Y.M., Xu, G., Ren, W.M., and Zhang, W. (2002). Dynamic response analysis of liquid-filled tanks. Engineering Mechanics, 19(4): 29-31, DOI: 1000-4750 (2002) 04-029-04.
15) Lv, X.L., Jin, G.F., and Wu, X.H. (1999). Reinforced concrete structure nonlinear finite element theory. Shanghai: Tongji University Press.
16) Mirzabozorg, H., Hariri ardebili, M.A., and Nateghi, A.R. (2012). Free surface sloshing effect on dynamic response of rectangular storage tanks. American Journal of Fluid Dynamics, 2(4): 23-30,DOI: 10.5923/j.ajfd.20120204.01.

17) Malhotra, P.K., Nimse, P., and Meekins, M. (2014). Seismic sloshing in a horizontal liquid storage tank. Structural Engineering International: Journal of the International Association for Bridge and Structural Engineering (IABSE), 2 4(4): 466-473, DOI:http:// dx .doi.org/10.2749/101686614X13854694314928.
18) Moeindarbari, H., Malekzadeh M., and Taghikhany T. (2014). Probabilistic analysis of seismically isolated elevated liquid storage tank using multi-phase friction bearing. Earthquakes and Structures, An International Journal, 6(1): 111-125, DOI:http:// dx.doi.org/10.12989/eas.2014.6.1.111.
19) Souli, M., and Zolesio, J.P. (2001). Arbitrary Lagrangian-Eulerian and free surface methods in fluid mechanics. Computer Methods in Applied Mechanics and Engineering, 191(3-5): 451-466, DOI:10.1016/S0045-7825 (01) 00313-9.
20) Shi, N., Ju, J., Xiaochuan, Y., and Huang, Y. (2012). Dynamic buckling analysis on fluid–solid coupling of large liquid storage tank. American Scientific Publishers, 10, (1-2): 131-137.
21) Tao, H. (2015). Partitioned coupling strategies for fluid-structure interaction with large displacement: Explicit, implicit and semi-implicit schemes. Wind and Structures, 20 (3): 423-448, DOI: 10.12989/was.2015.20.3.423.
22) Yazici, G. (2014). Parametric study of the seismic response of base isolated liquid storage tanks with lead-core Elastomeric bearings. Acta Physica Polonica A, 125(2): 382-284. DOI: 10.12693/ APhysPolA.125.382.
23) Yue, B.Z., Liu, Y.Z., and Wang, Z.L. (2001). ALE finite element method for three-dimensional large amplitude liquid sloshing using fractional step method. Chinese Journal of Applied Mechanics, 18(1): 110-115, DOI: 1000-4939 (2001) 01-0110-06.
24) Zhang, L.X., Tan, X.J., Liu, J.P., and Zhong, J.R. (2011). Seismic response analysis of large liquid storage tank considering fluid-structure interaction. Advanced Materials Research, 368-373:983-987, DOI: 10.4028/ www.scientific.net/AMR.368-373.983.
25) Zhang, R.F., Weng, D.G., and Ge, Q.Z. (2014). Shaking table experiment on a steel storage tank with multiple friction pendulum bearings.Structural Engineering and Mechanics, 52(5): 875-887, DOI: 10.12989/sem.2014.52.5.875.
26) Zheng, M.J., Wang, W.J., Chen, Z.N., and Wu, L.J. (2003). Determination for mechanical constants of rubber Mooney-Rivlin model. China Rubber Industry, 8:462-466, DOI: 1000-890X (2003) 08-0462-04.